Draft global O_2 and Atmospheric Potential Oxygen (APO) budgets

Deliverable 1.1

Authors: Nicolas Mayot, Corinne Le Quéré and Andrew Manning

This project received funding from the Horizon 2020 programme under the grant agreement No. 821003.

Document Information

GRANT AGREEMENT	821003
PROJECT TITLE	Climate Carbon Interactions in the Current Century
PROJECT ACRONYM	4C
PROJECT START DATE	1/6/2019
RELATED WORK PACKAGE	W1
RELATED TASK(S)	T1.1.1
LEAD ORGANIZATION	UEA
AUTHORS	Nicolas Mayot, Corinne Le Quéré, Andrew Manning
SUBMISSION DATE	30/11/2020
DISSEMINATION LEVEL	PU / CO / DE

History

DATE	SUBMITTED BY	REVIEWED BY	VISION (NOTES)
23/11/2020	Nicolas Mayot (UEA)	Pierre Friedlingstein (UNEXE)	

Please cite this report as: Mayot, N., Le Quéré, C. and Manning, A. (2020), Draft global O_2 and Atmospheric Potential Oxygen (APO) budgets, D1.1 of the 4C project

Table of Contents

List of tables

List of figures

About 4C

Climate-Carbon Interactions in the Coming Century (4C) is an EU-funded H2020 project that addresses the crucial knowledge gap in the climate sensitivity to carbon dioxide emissions, by reducing the uncertainty in our quantitative understanding of carbon-climate interactions and feedbacks. This will be achieved through innovative integration of models and observations, providing new constraints on modelled carbon-climate interactions and climate projections, and supporting Intergovernmental Panel on Climate Change (IPCC) assessments and policy objectives.

Executive Summary

Natural and anthropogenic processes influencing carbon dioxide (CO_2) accumulation in the atmosphere also induce changes in atmospheric concentration of oxygen (O_2). Measurements of CO_2 and O_2 atmospheric concentrations can be combined into a unique tracer named 'Atmospheric Potential Oxygen' (APO) that is only sensitive to air-sea gas exchange and fossil fuel burning processes. In our contemporary global APO budget analysis (from 1992 to 2018), done with observational-based products, the influence of fossil fuel burning is isolate in order to study air-sea exchanges of APO. Our current understanding of oceanic processes can be evaluated by comparing calculated year-to-year variations in air-sea exchanges of APO with similar estimates from global ocean biogeochemistry models.

Keywords

oxygen, global budget, observations, air-sea exchanges, interannual variabilities.

1 Introduction

There are three major processes influencing the CO_2 accumulation in the atmosphere (Figure 1): fossil fuel burning (CO2 source), land uptake (CO2 sink) and ocean uptake (CO2 sink). All of them induce variations in atmospheric O_2 concentration too. Therefore, when studying O_2 fluxes, some information about processes impacting the CO_2 cycle can be gained. For two processes, fossil fuel burning and land uptake, molar exchange ratios of CO_2 and O_2 could be considered constant (i.e., α_B and α_F). In contrast, air-sea exchanges of CO_2 and O_2 are, to a certain extent, decoupled from each other. It is due to the inorganic carbon chemistry in the ocean and oceanic biological and circulation processes that lead to opposing exchanges of O_2 and CO_2.

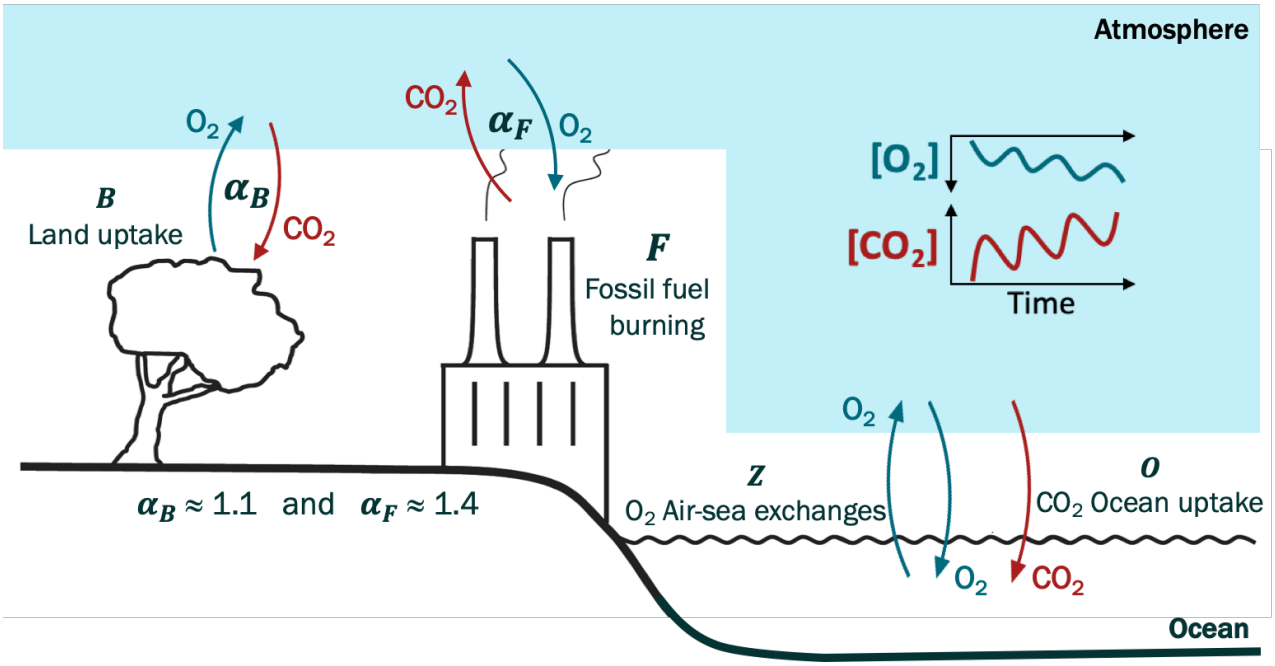

Figure 1. The dominant controls on the long-term trends in atmospheric concentration of O_2 and CO_2. Modified from Keeling and Manning (2014) in Treatise on Geochemistry (Second Edition), p. 385-404.

Atmospheric concentrations of O_2 and CO_2 can be combined to form an Atmospheric Potential Oxygen (APO) tracer by using α_B, the O_2:CO_2 molar exchange ratio for land uptake: APO = O_2 + α_B x CO_2. By design, the land biotic process does not influence APO variations. A modification in APO concentration can only be induce by changes in fossil fuel burning and gas exchange at the air-sea interface. However, reliable estimates about the quantity of burned fossil fuel exist in order to focus on oceanic fluxes (i.e., ***Z*** and ***O*** in Figure 1).

As part of the WP1, we are improving our understanding of processes controlling the contemporary CO_2 cycle by building global APO and O_2 budgets with an approach similar to the one used for the global carbon budget. The quantification of each flux that influences the atmospheric concentration of O_2 and APO is done with the

most recent datasets. Those global, as well as regional, budgets will provide estimates of ocean and land fluxes that models should reproduced and will be used to identify the origin of the carbon budget imbalance.

2 Methods and data

2.1 Global budget equations

As explained in introduction, APO is a tracer that combines atmospheric O_2 and CO_2 concentrations. Global changes in atmospheric concentrations of O_2 (ΔO_2), CO_2 (ΔCO_2) and APO (ΔAPO) can be represented by,

$$\Delta O_2 = -\alpha_F F + \alpha_B B + Z \quad (1)$$

$$\Delta CO_2 = F - O - B \quad (2)$$

$$\Delta APO = \Delta O_2 + \alpha_B \Delta CO_2 = (-\alpha_F + \alpha_B)F - \alpha_B O + Z \quad (3)$$

Where ***F*** is the atmospheric CO_2 emitted from fossil fuel combustion, ***B*** is the land biotic CO_2 sink, ***Z*** is the net exchange of atmospheric O_2 with the oceans and ***O*** is the oceanic CO_2 sink. Coefficients α_F and α_B are estimates of O_2:CO_2 molar exchange ratios for fossil fuel combustion and land biota, respectively. Global budget analyses are performed by evaluating if measured values of annual global changes in atmospheric concentrations of APO and O_2 (see below) matches estimated values obtained by using observational-based estimates of components ***F***, ***O*** and ***Z*** (i.e., ***B*** is computed from equation 2).

Measured changes in APO concentration is the combination of observed changes in O_2 and CO_2 concentrations. The CO_2 concentration is reported in ppm (parts per million, the number of CO_2 molecules per million air molecules) and noted X_{CO2}. For atmospheric O_2, changes in concentration are measured as changes in the O_2/N_2 ratio relative to a fixed reference,

$$\delta(O_2/N_2) = \frac{(O_2/N_2)_{measured}}{(O_2/N_2)_{reference}} - 1 \quad (4)$$

Because changes in $\delta(O_2/N_2)$ are very small, $\delta(O_2/N_2)$ values are multiplied by 10^6 and expressed in 'per meg' units (ppm changes in a ratio). The measured changes in APO concentration (δAPO, in per meg) is obtained by combining measured changes in $\delta(O_2/N_2)$ and X_{CO2},

$$\delta APO = \delta(O_2/N_2) + [\alpha_B(X_{CO2} - 350)]/X_{O2} \quad (5)$$

Where 350 is an arbitrary reference, α_B converts ppm of CO_2 into ppm of O_2 and X_{O2} = 0.2095, the atmospheric O_2 mole fraction, converts ppm of O_2 into per meg units.

Global APO and O_2 budgets are done by focusing on annual changes in δAPO and $\delta(O_2/N_2)$, expressed in per meg/yr, that can be represented by equations,

$$\Delta(\delta APO) \times (M_{air}.X_{O2}) = (-\alpha_F + \alpha_B)F - \alpha_B O + Z - \frac{\Delta N_2.X_{O2}}{X_{N2}} \quad (6)$$

$$\Delta(\delta(O_2/N_2)) \times (M_{air}.X_{O2}) = -\alpha_F F + \alpha_B B + Z - \frac{\Delta N_2.X_{O2}}{X_{N2}} \quad (7)$$

Where $\Delta(\delta APO)$ and $\Delta(\delta(O_2/N_2))$ are converted in Tmol O_2/yr by using X_{O2} and M_{air} = $1.769.10^{20}$, the total moles of dry air. The last right end side component in equations 6 and 7 represents the net effect of oceanic N_2 outgassing on measured $\Delta(\delta(O_2/N_2))$. The two terms for oceanic sources of O_2 and N_2 can be combined together and corrected for additional O_2 outgassing from the ocean due to the deposition of excess anthropogenic reactive nitrogen,

$$Z_{eff} = Z - \frac{\Delta N_2.X_{O2}}{X_{N2}} + Z_{anthN} \quad (8)$$

2.2 Datasets available

2.2.1 Atmospheric observations from land stations

Observations of atmospheric O_2 and APO concentrations are from air samples collected at nine land stations (Table 1) which are part of the Scripps O_2 program (https://scrippsO2.ucsd.edu). Air samples are collected twice a month to evaluate $\delta(O_2/N_2)$ and δAPO. Data are available at nine stations since 1997, before data were only available at three (since 1992) or five stations (since 1994). Based on these observations and for each station, a monthly time series was calculated. Each time series had a quasi-regular seasonal cycle that was removed by subtracting from the original time series a climatological seasonal cycle obtained after the long-term trend had been removed with a third-order polynomial.

A global mean APO time series was computed using a weighted average of individual deseasonalized monthly time series, with weights based on the latitudinal location of each station and the area between latitude circles (Table 1). Annual changes in atmospheric O_2 and APO concentrations were estimated by taking the difference between averaged concentrations from October to March. This 6-months average was used to remove low-frequency variabilities.

Table 1. Station names and locations. Weightings used in constructing the global mean APO time series are listed for different station combinations.

Station name	Latitude (°N)	Longitude (°E)	Global station weightings		
			5 stations (1992-93)	7 stations (1994-96)	9 stations (1997-18)
Alert	82.45	−62.52	0.12	0.05	0.05
Cold Bay	55.20	−162.72		0.11	0.11
La Jolla	32.87	−117.25	0.16	0.12	0.12
Mauna Loa	19.53	−155.58			0.10
Kumukahi	19.52	−154.82	0.20	0.20	0.10
Samoa	−14.25	−170.57	0.24	0.24	0.24
Cape Grim	−40.68	144. 68	0.28	0.17	0.17
Palmer Station	−64.92	−64.00		0.11	0.09
South Pole	−89.98	−24.80			0.02

2.2.2 Fossil-fuel burning estimates

Estimates of global annual CO_2 emissions (in $TgCO_2$/yr) from fossil-fuel burning are from the Global Carbon Budget project (GCP-GridFED version 2019.1, https://doi.org/10.5281/zenodo.3958283). Estimates of O_2 consumption were obtained by using a α_F value different for each fuel type: 1.44, 1.17, 1.95 and 0 for oil, coal, gas and the production of cement, respectively.

2.2.3 Oceanic CO_2 sink: pCO_2-based flux estimates

Estimates of global ocean CO_2 sink are from three pCO_2-based flux data products: Jena-MLS (http://www.bgc-jena.mpg.de/CarboScope/?ID=oc), MPI-SOMFFN (https://doi.org/10.7289/V5Z899N6) and CMEMS, used by the Global Carbon Budget project. All of these data-based products used measurements from the Surface Ocean CO_2 Atlas (SOCAT, https://www.socat.info/) and were corrected for a pre-industrial steady state source of CO_2 to the atmosphere from river input to the ocean (estimated to be 0.78 GtC/yr).

2.2.4 Oceanic sources of O_2 and N_2 to the atmosphere from global ocean heat content estimates

There are no direct measurements available about oceanic sources of O_2 to the atmosphere. One possibility would be to measure annual changes in the global oceanic O_2 inventory. However, spatiotemporal data coverage and measurement accuracy are insufficient. As an alternative, a relationship exists between long-term changes in oceanic O_2 inventory and net air-sea heat flux which allow to rewrite equation 8,

$$Z_{eff} = \left(\gamma_{O2} - \frac{X_{O2}}{X_{N2}}\gamma_{N2}\right) \times Q + Z_{anthN}$$

Where coefficients γ are natural gas flux/heat flux ratios (γ_{O2} = 4.9 nmol/J and γ_{N2} = 2.2 nmol/J) and Q is the annual net air-sea heat flux. The latter was based on the annual changes in global ocean heat content estimated from an average of three data-based products that evaluated warming rates at ocean depths from 0 to 2000 m:

- JMA (https://www.data.jma.go.jp/gmd/kaiyou/english/ohc/ohc_data_en.html)
- NCEI (https://www.nodc.noaa.gov/OC5/3M_HEAT_CONTENT/heat_global.html)
- IAP (http://159.226.119.60/cheng/)

The term Z_{anthN} has been estimated at 10.38 $TmolO_2$/yr from a global modelling analysis.

3 Draft of global APO and O_2 budgets and ongoing work

3.1 Global APO budget and uncertainties

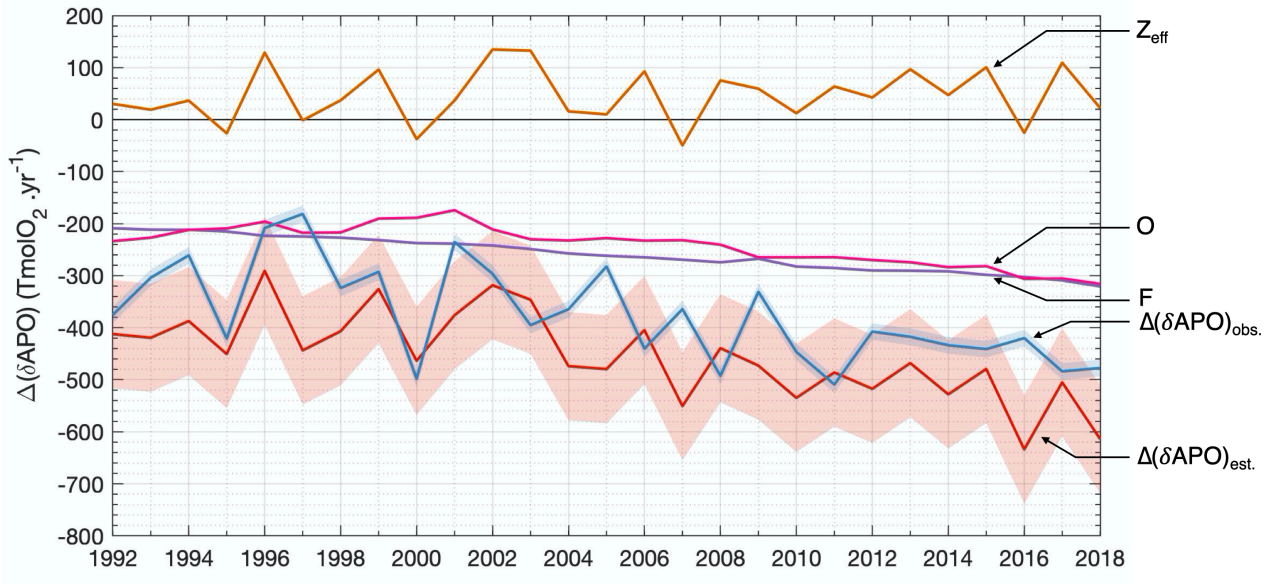

Figure 2. Combined components of the global APO budget illustrated in Fig. 1 as a function of time. All time series are in Tmol O_2/yr, which means that coefficients α_F and α_B have been applied (equation 6). Shaded areas illustrate uncertainties of the observed and estimated $\Delta(\delta APO)$ (Table 2).

As expected, there is a long-term negative trend in global mean APO (Figure 2), that decreased from -375 Tmol/yr in 1992 to -478 Tmol/yr in 2018.This is mostly induce by the negative trend in the fossil fuel burning process (***F***) that also increases the CO_2 ocean uptake (***O***). The observed global mean APO is lower than the sum of ***F*** and ***O***, because there is a global oceanic outgassing of O_2 into the atmosphere of 41 Tmol/yr on average. When all components of the budget are added together, the estimated global mean APO is slightly lower than the observed value. The mean budget imbalance between 1992 and 2018 is on average -79 Tmol/yr and has no trend (not statistically different from 0). The highest source of uncertainty (Table 2) on the estimated APO arises from the α_B parameter (± 75 Tmol/yr). On the opposite side, the uncertainty on the component ***F*** has the lowest effect on the budget (± 13 Tmol/yr).

The observed interannual variability in APO is around 93 Tmol/yr (1σ). Estimated interannual variabilities in ***F*** and ***O*** are relatively small, less than 38 Tmol/yr. Therefore, a large part of the interannual variability in APO is probably linked to the oceanic outgassing (Z_{eff}). The estimated interannual variability in Z_{eff} time series (Figure 2) is induced by interannual variabilities in net air-sea heat-flux (Q). However, it has been demonstrated that year-to-year variations in Q are not always related to changes in oceanic O_2 outgassing.

Table 2. Estimates of uncertainties associated with components of the global APO budget, as well as their effect on the estimated $\Delta(\delta(O_2/N_2))$.

Parameter	Uncertainty	Effect on estimated Δ(δAPO)
α_B	± 0.1	± 75 TmolO_2/yr
α_F	± 0.04 (gas) ± 0.03 (oil) ± 0.03 (coil)	± 27 TmolO_2/yr
F	± 5%	± 13 TmolO_2/yr
O	± 0.6 PgC/yr	± 55 TmolO_2/yr
Z_{eff}	± 100%	± 36 TmolO_2/yr
	Quadrature sum of all uncertainties:	± 104 TmolO_2/yr

3.2 Global O_2 budget and uncertainties

There is a long-term negative trend in global mean O_2 (Figure 3), that decreased from -497 Tmol/yr in 1992 to -1019 Tmol/yr in 2018. As for APO, this is mostly due to the negative trend in the fossil fuel burning process (F). The land biotic and oceanic outgassing components are both adding some O_2 to the atmosphere, on average 104 Tmol/yr and 47 Tmol/yr, respectively. When all components of the O_2 budget are added together, the estimated global mean O_2 is largely lower than the observed value. The mean budget imbalance between 1992 and 2018 is on average -347 Tmol/yr and has a negative trend of -5 Tmol/yr. The reasons for such high budget imbalance in this draft of O_2 budget will be investigated. The highest source of uncertainty (Table 3) on the estimated O_2 arises from the ***O*** parameter (± 51 Tmol/yr) which is used to derive the land biotic component following equation 2. On the opposite side, the uncertainty on the α_B parameter (± 8 Tmol/yr) has the lowest effect on the budget. Our objective is to reduce the current budget imbalance in the O_2 budget, as well as to use observational-based estimates for the land biotic component.

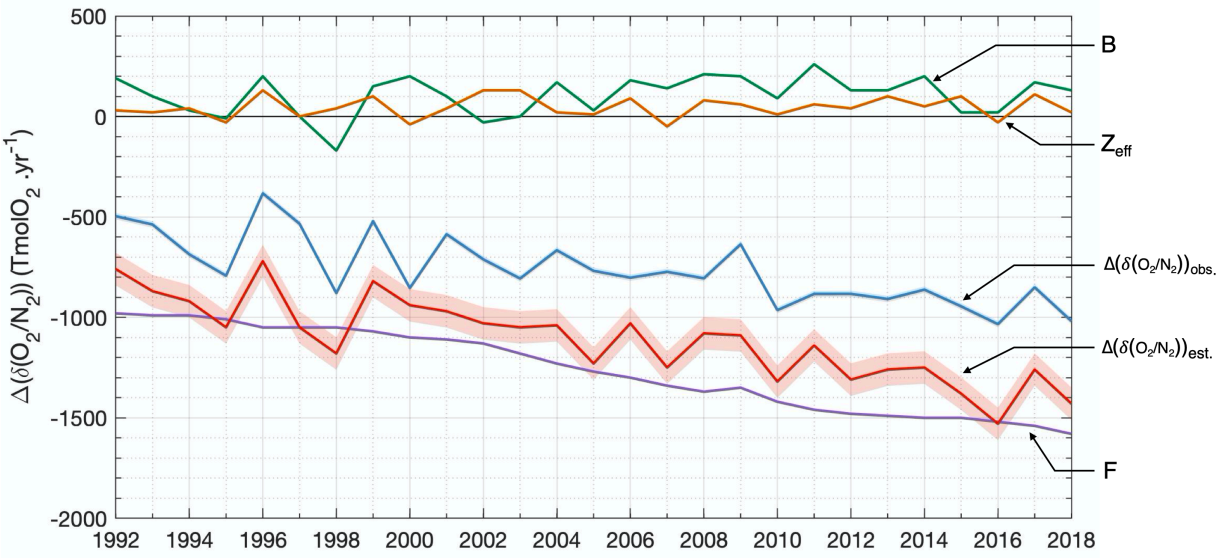

Figure 3. Combined components of the global O_2 budget illustrated in Fig. 1 as a function of time. All time series are in Tmol O2/yr, which means that coefficients α_F and α_B have been applied (equation 7). Shaded areas illustrate uncertainties of the observed and estimated $\Delta(\delta(O_2/N_2))$ (Table 3).

Table 3. Estimates of uncertainties associated with components of the global O_2 budget, as well as their effect on the estimated $\Delta(\delta(O_2/N_2))$.

Parameter	Uncertainty	Effect on estimated $\Delta(\delta(O_2/N_2))$
α_B	± 0.1	± 8 $TmolO_2$/yr
α_F	± 0.04 (gas) ± 0.03 (oil) ± 0.03 (coil)	± 26 $TmolO_2$/yr

F	± 5%	± 29 TmolO_2/yr
O	± 0.6 PgC/yr	± 51 TmolO_2/yr
Z_{eff}	± 100%	± 47 TmolO_2/yr
dAPO	± 0.17 PgC/yr	± 14 TmolO_2/yr
	Quadrature sum of all uncertainties:	± 81 TmolO_2/yr

3.3 Regional analysis and model evaluations

Fluxes of air-sea APO exchange can be calculated with an atmospheric transport inversion method that uses the atmospheric observations from land stations with an atmospheric tracer transport model. Such calculated fluxes allow to obtain a global estimate for ***Z***, as well as regional contributions: tropics (30S-30N), northern extratropic and southern extratropic. Daily maps of air-sea APO exchanges between 1994 and 2019 were downloaded from: http://www.bgc-jena.mpg.de/CarboScope/?ID=apo (Jena CarboScope inversion product).

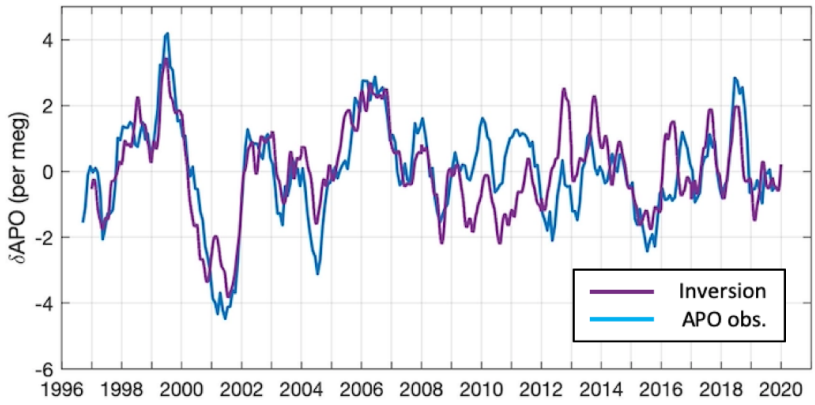

Figure 4. Comparison between observed and estimated (from inversion method) global mean APO time series. The long-term trend and seasonal cycle have been removed.

A quick comparison between observations and inversion results for δAPO (figure 4) demonstrated that the inversion method is able to reproduce some observed interannual variabilities in the APO signal. Most of this interannual variability is linked to air-sea O_2 exchanges (***Z***, data not shown). Maps produced by the inversion method could be used to study each oceanic region influences the interannual variabilities in observed δAPO. Based on those results, the influence of some oceanic processes could be suggested, for example, vertical mixing and biological production, and studied with in situ and remote sensing datasets.

Five modelling teams, involved in the Global Carbon Budget 2020, are contributing to this analysis by providing monthly maps of air-sea O_2 exchanges. Those models are compared to each other and to the inversion results

(Figure 5). Global ocean biogeochemistry models produced air-sea O_2 fluxes values two times lower than expected from inversion results. However, global and regional interannual variabilities were observed in all models and inversion results. This is an example about how APO observations could help to identified important oceanic regions and processes that might impact air-sea CO_2 fluxes.

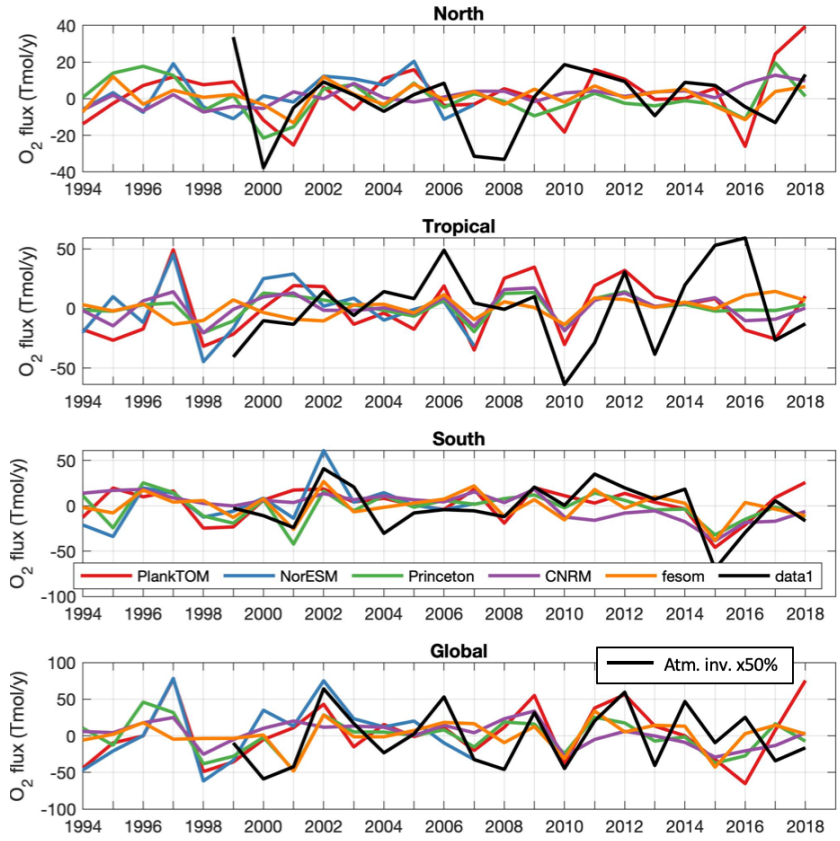

Figure 5. Annual changes in air-sea O_2 fluxes estimated by five global ocean biogeochemistry models and by the inversion method. Estimates from three oceanic regions: north (>30N), tropical (30S-30N) and South (<30S); are combined to calculate a global value.